

# A theoretical study on drop impact sound and rain noise

By Y. P. GUO† AND J. E. FLOWCS WILLIAMS

Department of Engineering, University of Cambridge, Trumpington Street,  
Cambridge CB2 1PZ, UK

(Received 23 May 1990)

This paper examines the sound waves generated when a spherical water drop impacts upon an initially quiescent water surface. The pressure fluctuations and the acoustic energy radiated by the initial impact are calculated analytically. It is shown that the rapid momentum exchange between the fluid in the falling drop and that in the main water body causes the radiation of compressive waves. These waves are radiated in the form of a wave packet with a densely packed edge which is heard in the far field as a noisy shock-like pulse followed by a quickly decreasing tail. The wave packet carries with it sound energy proportional to the kinetic energy of the falling drop and to the cube of the impact Mach number. Applications of these analytic results to the study of noise from natural rain are discussed, and an illustrative example is given where the noise level due to rain showers is linearly related to the rainfall rate, which is shown to be consistent with observations.

---

## 1. Introduction

On account of its relevance to noise generation by rain showers, the phenomenon of a water droplet falling onto a flat water surface has attracted much research in recent years (e.g. Nystuen 1986; Pumphrey, Crum & Bjorno 1989; Oğuz & Prosperetti 1990). These studies suggest that a falling droplet causes acoustic radiation essentially through two mechanisms, namely the initial impact and the subsequent entrainment and pulsations of air bubbles. While the sound associated with bubbles has been quite extensively studied over the past few decades (see, for example, Minnaert 1933; Strasberg 1956; Plesset & Prosperetti 1977), the initial impact sound is less satisfactorily understood, though it has long been conjectured to be an appreciable component of the noise generated by rain showers (Franz 1959; Wenz 1962). This is probably due to the highly transient nature and the extremely short timescale of the initial impact process, which makes both experimental observations and numerical simulations difficult. It is therefore desirable to establish analytical models that are simple enough to allow for analytical solutions, but yet reveal basic features of the sound associated with the impact process. This paper presents such a model.

There is evidence that the spectral peak of rain noise at about 15 kHz is dominantly produced by bubbles entrained by rain drops in a very narrow band of the drop size distribution (Pumphrey *et al.* 1989), and because of this, the amplitude of the spectral peak is not well correlated with the rain conditions such as wind

† Present address: Department of Ocean Engineering, MIT, Cambridge, MA 02139, USA.

speeds and rainfall rates (Prosperetti, Crum & Pumphrey 1989). However, the overall noise levels of rain showers have been observed to be strongly dependent on these conditions; variations in wind speeds and rainfall rates significantly change the noise level. For example, it has been observed that increases in the rate of rainfall increase the general level of the noise spectrum, particularly those relatively flat parts away from the sharp bubble-associated peak (Nystuen 1986; Scrimger *et al.* 1989). This gives grounds for suggesting that, though the bubbles are responsible for the spectral peak, the overall noise level in strong winds and moderate or heavy rain is probably associated with processes other than the entrainment of bubbles. The initial impact is obviously a very likely candidate. In this paper, we examine how sound is generated when the impact occurs and how much sound is radiated during the impact.

To this end, we consider a single spherical water drop falling onto an initially quiescent water surface. During the initial impact, the main mechanism of acoustic radiation is identified as the rapid momentum exchange between the fluid in the falling drop and that at rest in the main body of water. As the fluid in the falling drop impacts on the still water, momentum is imparted to the water body while the drop deforms and slows down. This process takes place over an extremely short interval, the momentum transfer being accomplished by the radiation of compressive waves which eventually escape to the far field as sound. These waves mostly emanate from the contact circle between the drop and the water surface during the initial period when the contact circle expands supersonically. Once the expanding contact circle becomes subsonic, the falling process only furnishes weak acoustic sources because some waves overtake the contact circle, accelerating the fluid ahead of it which is brought into motion before it is hit by the falling fluid. This reduces the velocity difference between the two groups of fluid elements before the impact, and hence, renders the momentum exchange after the impact much more gradual and less well coupled to sound.

Pressure waves due to the initial impact are calculated analytically in this paper and it is shown that they have amplitudes of the order  $\rho_0 cU$ , where  $\rho_0$  and  $c$  are respectively the constant mean density and sound speed in water, and  $U$  is the drop impact velocity. This is analogous to the classic water hammer phenomenon and has been noticed by Nystuen (1986) in his numerical calculations. In experiments and numerical simulations, the pressures are usually observed to be less than, though of the same order as,  $\rho_0 cU$ . We will show that this is due to the three-dimensional propagation effects and is not associated with the impact dynamics. Locally, the impact is precisely the same as a one-dimensional water hammer; the pressure waves are all launched with amplitude  $\rho_0 cU$ , but because they have to propagate away from their source in a three-dimensional space, their amplitudes decay owing to spherical spreading. We will show that these waves form a wave packet with a densely packed edge which is heard in the far field as a noisy shock-like pulse followed by a rapidly decreasing tail. The extremely short scale of this wave packet suggests its relevance to the relatively flat parts in the noise spectrum observed in natural rains.

To see how much sound is radiated during the initial impact, we calculate the radiated acoustic energy and find that it is proportional to the kinetic energy carried by the falling drop and to the cube of the impact Mach number  $M = U/c$ , for small values of  $M$ , which is usually the case for drops in natural rains where  $M$  is of the order  $10^{-2}$  to  $10^{-3}$ . The cubic dependence on the impact Mach number of the radiation efficiency indicates the dipole nature of the acoustic source (Lighthill 1952) and has been confirmed by Franz (1959) in his experimental studies. Using this

result, we will demonstrate that the noise level from rain showers can be related to parameters such as rainfall rates, by incorporating experimental data on the drop size distribution. A simple example is given where the most energetic drops in a shower are assumed to have an identical effective size. This illustrative example shows that the sound intensity is a linear function of the rainfall rate, a result which we have derived before (Guo 1986) from a general theory based on dimensional analysis, which was shown to be consistent with measurements (Nystuen 1986) in both the functional dependence between sound level and rainfall rate and the absolute decibel levels (see also Scrimger *et al.* 1989).

## 2. Formulation

Though the process of a droplet falling onto a water surface is very complicated, the acoustic radiation associated with the initial impact can be examined in a very simple way by making use of the Kirchhoff theorem, which states that the pressure fluctuations at the observation position  $\mathbf{x}$  at time  $t$  can be expressed in terms of a retarded integral of the normal velocity distribution over a control surface (see, for example, Dowling & Ffowcs Williams 1983). We choose the initially undisturbed water surface as the control surface with a Cartesian coordinate system  $(x_1, x_2, x_3)$  fixed such that the control surface coincides with the plane  $x_3 = 0$ . A droplet of spherical shape with radius  $a$  is assumed to be falling in the negative  $x_3$  direction with constant velocity  $U$ , and it touches the water surface at the origin of the coordinate system at  $t = 0$ . The geometry is illustrated in figure 1. Denoting by  $u_3(x_\alpha, t)$  the velocity distribution in the negative  $x_3$  direction on the control surface  $x_3 = 0$ , the Kirchhoff theorem then gives the pressure fluctuations  $p(\mathbf{x}, t)$  as

$$p(\mathbf{x}, t) = \frac{\rho_0}{2\pi} \frac{\partial}{\partial t} \int_{y_\alpha} \frac{u_3(y_\alpha, \tau)}{|\mathbf{x} - \mathbf{y}|} d^2y_\alpha, \tag{2.1}$$

where  $\rho_0$  is the constant mean density in water and the integrals are performed on the plane  $y_3 = 0$  at the retarded time  $\tau = t - |\mathbf{x} - \mathbf{y}|/c$ ,  $c$  being the constant sound speed in water and  $|\mathbf{x} - \mathbf{y}|$  the modulus of  $\mathbf{x} - \mathbf{y}$ . Since the only time dependence in the integrand is contained in  $\tau$ , the derivative with respect to  $t$  can be transferred inside the integrals and converted to one with respect to  $\tau$ . We can then rewrite (2.1) as

$$p(\mathbf{x}, t) = \frac{\rho_0}{2\pi} \int_{y_\alpha} \frac{1}{|\mathbf{x} - \mathbf{y}|} \frac{\partial u_3(y_\alpha, \tau)}{\partial \tau} d^2y_\alpha. \tag{2.2}$$

To evaluate this, it is necessary to specify the velocity distribution  $u_3(x_\alpha, t)$ . It can be noted that, during the initial impact, this velocity distribution is non-zero only within the contact circle between the drop and the water surface because the contact circle expands supersonically. Denoting by  $b(t)$  the radius of the drop/surface contact circle, we find from the geometry of the problem that

$$b(t) = [a^2 - (a - Ut)^2]^{\frac{1}{2}}, \tag{2.3}$$

from which the expanding velocity of the circle can be derived by differentiation as

$$\dot{b}(t) = \frac{(a - Ut) U}{[a^2 - (a - Ut)^2]^{\frac{1}{2}}}, \tag{2.4}$$

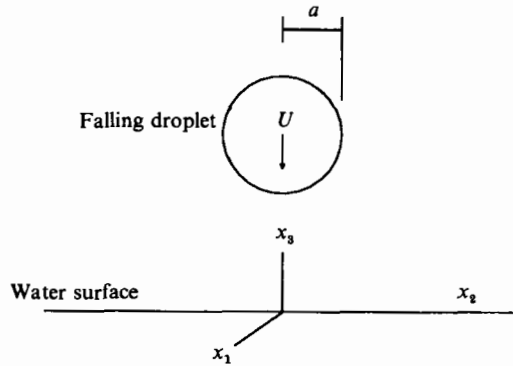


FIGURE 1. Water droplet falling onto an originally quiescent water surface.

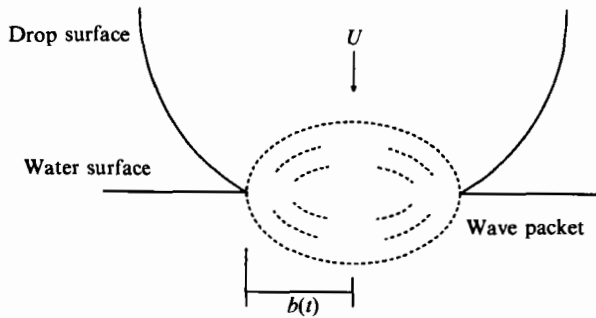


FIGURE 2. The wave packet produced by the supersonically expanding contact circle.

where the dot denotes a time derivative. This is larger than the constant sound speed  $c$  for small time. The instant  $t_c$  at which  $\dot{b}$  becomes smaller than  $c$  is given by

$$t_c = \frac{a}{U} \left( 1 - \frac{1}{(1+M^2)^{\frac{1}{2}}} \right) \sim \frac{1}{2} M^2 \frac{a}{U} \quad \text{for } M \ll 1, \tag{2.5}$$

where  $M = U/c$  is the small impact Mach number.

During the initial impact, since no waves can travel ahead of the supersonically expanding contact circle, the waves form a wave packet within the region inside the contact circle  $|x_\alpha| < b(t)$ , as schematically shown in figure 2. These waves are not aware of any boundary effects so that they are completely anti-symmetrical about the plane  $x_3 = 0$ ; the velocity within the wave packet varies continuously from zero at the edge of the packet in the water body to the constant value  $U$  at the edge in the drop. Thus, the velocity distribution on the median plane must be half the velocity difference  $U$ . It should be pointed out that this is true only for  $t < t_c$  when  $\dot{b}$  is greater than  $c$ ; when  $\dot{b}$  becomes subsonic, some waves may overtake the expanding contact circle, be reflected by the pressure release surface ahead of the contact circle, and hence, destroy the complete axisymmetry. However, the process taking place when  $t > t_c$  is much less significant in radiating sound waves. Therefore, the velocity distribution  $u_3(x_\alpha, t)$  can be written as

$$u_3(x_\alpha, t) = \frac{1}{2} U H(t) H(b(t) - |x_\alpha|), \tag{2.6}$$

where  $H$  is the Heaviside step function, equal to unity for positive arguments and zero otherwise. It is now constructive to compare this result with that in the classic

one-dimensional water hammer theory where a quiescent water column is hit by another falling column. When this occurs, two waves are produced by the impact, one travelling into the quiescent water and the other into the falling column. As a result, the velocity jumps by half of the impact velocity every time a wave is passed, which gives the velocity between the two waves everywhere to be precisely half the impact velocity. In our case of a falling droplet, the velocity within the wave packet is not everywhere equal to  $\frac{1}{2}U$  because of the three-dimensional spreading effects. However, the properties of these axisymmetrical waves ensure that the velocity on the median plane is exactly half the impact velocity.

On substituting (2.6) into the Kirchhoff formulation (2.2), it immediately follows that

$$p(\mathbf{x}, t) = \frac{\rho_0 U}{4\pi} \int_{y_\alpha} \frac{1}{|\mathbf{x} - \mathbf{y}|} \frac{\partial b(\tau)}{\partial \tau} H(\tau) \delta(b(\tau) - |y_\alpha|) d^2 y_\alpha, \tag{2.7}$$

where  $\delta$  is the Dirac delta function resulting from the derivative of the Heaviside function. The  $y_\alpha$  integrals can be conveniently evaluated by changing the integration variable to polar coordinates according to  $y_1 = \lambda \cos \alpha$  and  $y_2 = \lambda \sin \alpha$ , and performing the  $\alpha$ -integral by making use of the properties of the  $\delta$ -function (Jones 1982). When this is done, the pressure fluctuations can be found to be

$$p(\mathbf{x}, t) = \frac{\rho_0 U c}{\pi} \int_0^{b(t)} \frac{H[4\lambda^2 x_\alpha^2 - (|\mathbf{x}|^2 + \lambda^2 - h^2)^2]}{[4\lambda^2 x_\alpha^2 - (|\mathbf{x}|^2 + \lambda^2 - h^2)^2]^{\frac{1}{2}}} \lambda d\lambda, \tag{2.8}$$

where, as a shorthand,  $h = [Ut - a + (a^2 - \lambda^2)^{\frac{1}{2}}]/M$ . It should be pointed out that care must be taken when evaluating this integral at positions close to the vertical axis where  $|x_\alpha| \rightarrow 0$ . In this case, the integration limits, determined by the Heaviside function in the integrand, approach each other so that the integral limits to zero if the integrand remains finite. However, when the quantity  $|\mathbf{x}|^2 + \lambda^2 - h^2$  also tends to zero, the integrand becomes unbounded, the integral in this case being non-zero and finite, as will become clear in the next section.

### 3. The pressure waves

The pressure waves radiated by the initial impact can now be examined through the result (2.8), which, after some straightforward changes of variables, can be rewritten as

$$\frac{p(\mathbf{x}, t)}{\rho_0 U c} = \frac{1}{\pi} \int_0^{\tilde{t}} \frac{(1 - M^2 \eta)}{\{4\tilde{x}_\alpha^2 \eta(2 - M^2 \eta) - [\tilde{x}^2 + \eta(2 - M^2 \eta) - (\tilde{t} - \eta)^2]^2\}^{\frac{1}{2}}} d\eta, \tag{3.1}$$

where the tildes mean non-dimensional quantities with the definitions

$$\tilde{t} = \frac{Ut}{aM^2}, \quad \tilde{\mathbf{x}} = \frac{\mathbf{x}}{aM}, \tag{3.2}$$

and the integration limits are also determined by requiring the argument in the square root to be positive, which comes from the Heaviside function in (2.8). The argument in the square root is a quartic polynomial in the integration variable  $\eta$ . Thus, according to the formula (3.148) of Gradshteyn & Ryzhik (1980), the integral is in principle expressible in terms of elliptic functions. It is also straightforward to evaluate it numerically; some results are shown in figure 3 where contours of

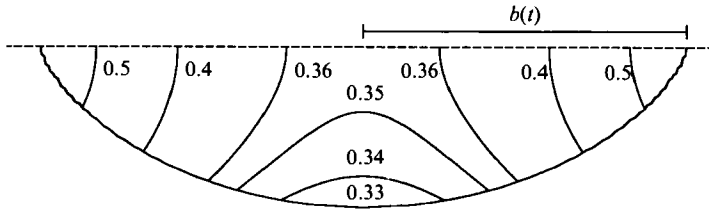


FIGURE 3. Contours of  $p(\mathbf{x}, t)/\rho_0 Uc$  within the wave packet.

$p(\mathbf{x}, t)/\rho_0 Uc$  are plotted in the  $(|x_a|, x_3)$ -plane, corresponding to the case of  $\tilde{t} = 0.5$  and  $M = 10^{-3}$ . Since the waves are axisymmetrical about the plane  $x_3 = 0$ , only half of the wave packet is plotted.

It can be seen from this figure that the compressive waves form a wave packet within the expanding circle  $|x_a| < b(t)$ . Close to the edge of the wave packet, the contours are densely packed, which indicates that the far field sound will be heard as a noisy shock-like pulse of very short duration. These are the typical characteristics of impact sound observed in experiments (e.g. Franz 1959). The values of the contours in figure 3 are all smaller than, but of the same order as, unity; The Waves have amplitudes of the order  $\rho_0 Uc$ , which is analogous to a one-dimensional water hammer, and is in agreement with the numerical calculations by Nystuen (1986). Note that the actual impact between the falling fluid elements and those at rest in the water occurs at the contact circle close to which the contour values are nearly unity. As the waves, generated with amplitude  $\rho_0 Uc$ , travel away from their source, namely the contact circle, the contour values decrease. The impact is locally exactly the same as the water hammer phenomenon, and the somewhat weaker pressure fluctuations observed in Nystuen's numerical calculations are due to the spreading effect; the effect is not related to any dynamics of the impact.

Now, we examine the pressure waves propagating along the  $x_3$  axis (namely, the axis where  $|x_a| = 0$ ), which is of particular interest because it is probably the most noisy direction; the far-field sound follows a dipole radiation pattern with its maximum on this axis. This feature is not clear from figure 3 because this figure only shows the wave pattern for small time  $t < t_c$ . When these compressive waves escape to the far field as sound, some of them must undergo reflections from either the drop surface or the surface of the water body, both of which are pressure-release surfaces, when they overtake the gradually expanding contact circle for  $t > t_c$ . However, since the reflected waves, and those much weaker waves produced by the subsonically expanding contact circle after the initial impact, can never overtake the waves which are directly generated by the initial impact and are propagating along the negative  $x_3$  axis down into the water body, the results obtained in the previous section could equally represent the actual far-field sound in this direction, with all the reflection effects only modifying the shape of the rapidly decaying tail that follows the initial noisy pulse.

To derive the pressures on the  $x_3$  axis, it is convenient to make use of the result (2.7), which, with  $|x_a|$  set to zero, assumes the form

$$p(\mathbf{x}, t) = \frac{\rho_0 Uc}{4\pi} \int_{y_2} \frac{1}{(x_3^2 + y_a^2)^{3/2}} \frac{\partial b(\tau)}{\partial \tau} H(\tau) \delta(b(\tau) - |y_a|) d^2 y_a, \tag{3.3}$$

where now  $\tau = t - (x_3^2 + y_a^2)^{1/2}/c$ . Similarly to the calculation of (2.7), we make the change of integration variables  $y_1 = \lambda \cos \alpha$  and  $y_2 = \lambda \sin \alpha$ . It is then clear that the integrand does not have any  $\alpha$ -dependence so that the  $\alpha$  integral is simply  $2\pi$ , and

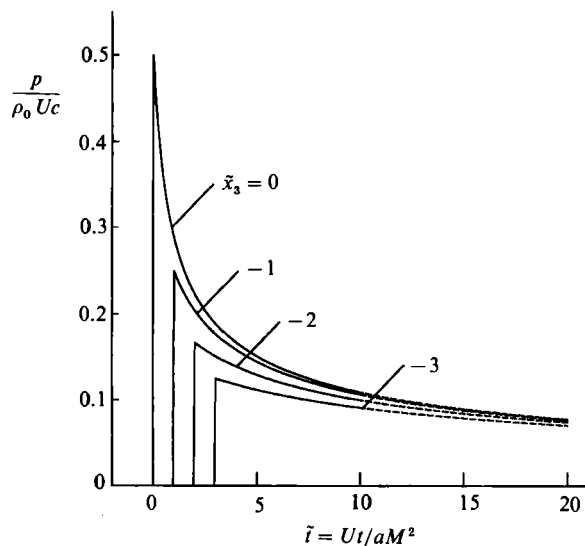


FIGURE 4. Pressures on the  $x_3$  axis as a function of time.

the  $\delta$ -function in the integrand can be utilized to carry out the  $\lambda$ -integration, which reduces (3.3) to

$$\frac{p(\mathbf{x}, t)}{\rho_0 U c} = \frac{1}{2(M^2 + 1)} \frac{1 - M^2 \tilde{t} + M^2 [1 + \tilde{x}_3^2 + 2\tilde{t} + M^2(\tilde{x}_3^2 - \tilde{t}^2)]^{\frac{1}{2}}}{[1 + \tilde{x}_3^2 + 2\tilde{t} + M^2(\tilde{x}_3^2 - \tilde{t}^2)]^{\frac{1}{2}}}, \quad (3.4)$$

where non-dimensional variables defined by (3.2) have been used.

Some results calculated from (3.4) are shown in figure 4; the shock-like initial pulse is evident, followed by a rapidly decreasing tail. The broken curves indicate the parts of the tails where it is not sufficient to use these results to represent the far-field sound. Both the drop surface and the surface of the water body are pressure-release surfaces with a reflection coefficient of  $-1$ . Thus the reflected waves have opposite sign to those coming directly from the impact; if these negative waves were taken into account, the tails shown in figure 4 would undoubtedly decrease to a negative value before forming the complete cycle observed in experiments and numerical simulations (e.g. Franz 1959; Nystuen 1986). It should be noted that the solid curves in figure 4 are not exact pressures; most parts of them will be modified by waves radiated after the initial impact. However, those waves are weak compared with the initial impact-generated shock-like pulses. Thus, the solid curves can be expected to give dominant contributions to the far-field sound.

#### 4. The radiated acoustic energy

As analysed in the previous section, the waves shown in figure 3 must undergo reflections from the boundary surfaces before they escape to the far field, so that the far-field radiation pattern can only be examined by including these reflection effects, which does not appear to be an easy task. However, the acoustic energy radiated to the far field can be calculated directly from the results derived in the previous sections without having to examine the far-field structure. This is because the energy radiated to infinity is precisely equal to the energy carried by the waves shown in figure 3 and represented by the result (2.8); the reflections only affect the form of the

pressure pulse. There is no mechanism in our model for this compressional energy, once it has been converted from the kinetic energy of the falling drop, to be converted back to kinetic energy again, so that it must all be radiated to the far field. Thus, the radiated acoustic energy can be calculated from the formula

$$E = 2 \int_0^{t_c} \int_{x_x} p(x_\alpha, 0, t) u_3(x_\alpha, t) dt d^2x_\alpha, \tag{4.1}$$

where  $u_3(x_\alpha, t)$  is the velocity distribution on the plane  $x_3 = 0$  specified by (2.6) and  $p(x_\alpha, 0, t)$  can be conveniently taken as (2.8) with  $x_3$  set to zero. The factor 2 in (4.1) takes account of the energy carried by those waves which originally propagate upwards into the droplet, but are later reflected back into the water body by the drop surface and eventually radiated to the far field.

On substituting (2.6) and (2.8) into (4.1), it follows that

$$E = \frac{\rho_0 U^2 c}{\pi} \int_0^{t_c} \int_0^{b(t)} \int_{x_x} \frac{H(b(t) - |x_\alpha|) H[4\lambda^2 x_\alpha^2 - (x_\alpha^2 + \lambda^2 - h^2)^2]}{[4\lambda^2 x_\alpha^2 - (x_\alpha^2 + \lambda^2 - h^2)^2]^{\frac{1}{2}}} \lambda d\lambda dt d^2x_\alpha, \tag{4.2}$$

$$= 2\rho_0 U^2 c \int_0^{t_c} \int_0^{b(t)} \int_0^{b(t)} \frac{H[4\lambda^2 r^2 - (r^2 + \lambda^2 - h^2)^2]}{[4\lambda^2 r^2 - (r^2 + \lambda^2 - h^2)^2]^{\frac{1}{2}}} \lambda d\lambda dr dt, \tag{4.3}$$

where the last step follows from changing the  $x_\alpha$  integrals to polar coordinates according to  $x_1 = r \cos \beta$  and  $x_2 = r \sin \beta$  with the  $\beta$ -integral equal trivially to  $2\pi$  since the integrand has no  $\beta$ -dependence. By making use of the formula (2.261) from Gradshteyn & Ryzhik (1980), the  $r$ -integral can be carried out, with the result

$$\int_0^{b(t)} \frac{H[4\lambda^2 r^2 - (r^2 + \lambda^2 - h^2)^2]}{[4\lambda^2 r^2 - (r^2 + \lambda^2 - h^2)^2]^{\frac{1}{2}}} r dr = \frac{1}{2} \arcsin \frac{r^2 - \lambda^2 - h^2}{2\lambda|h|} \Big|_A^B, \tag{4.4}$$

where the integration bounds  $A$  and  $B$  are jointly determined by the two inequalities

$$0 < r < b, \quad 4\lambda^2 r^2 - (r^2 + \lambda^2 - h^2)^2 > 0,$$

the latter of which results from the Heaviside function on the left-hand side of (4.4) and can be easily shown to be equivalent to

$$|\lambda - |h|| < r < \lambda + |h|.$$

Considering that the  $t$ -integral is from zero to  $t_c$  and that with respect to  $\lambda$  from zero to  $b(t)$ , it is straightforward to prove the relation

$$0 < |\lambda - |h|| < \lambda + |h| < b,$$

from which we can determine the integration limits  $A$  and  $B$  to be

$$A = |\lambda - |h||, \quad B = \lambda + |h|.$$

On substituting these into (4.4), the right-hand side of it reduces to  $\frac{1}{2}\pi$  and (4.3) becomes

$$E = \rho_0 U^2 c \pi \int_0^{t_c} \int_0^{b(t)} \lambda d\lambda dt = \frac{1}{2} \pi \rho_0 U^3 c t_c^2 (a - \frac{1}{3} U t_c).$$

Making use of (2.5) for  $t_c$ , this result can be rewritten in terms of the impact Mach number  $M$  as

$$\frac{E}{E_0} = \frac{1}{4M} \left( 2 + \frac{1}{(1+M^2)^{\frac{1}{2}}} \right) \left( 1 - \frac{1}{(1+M^2)^{\frac{1}{2}}} \right)^2, \tag{4.5}$$

$$\sim \frac{3}{16} M^3 \quad \text{for } M \ll 1, \tag{4.6}$$

where  $E_0$  is the kinetic energy carried by the falling drop, that is,

$$E_0 = \frac{4}{3}\rho_0 U^2 \pi a^3.$$

This result reveals that the acoustic energy radiated owing to the initial impact is proportional to the drop energy  $E_0$  and to the cube of the drop impact Mach number  $M$ , indicating the dipole nature of the radiation, as described by the Lighthill (1952) theory of noise production by flow processes. The cubic Mach-number dependence of the radiation efficiency has also been observed in the experiments of Franz (1959).

Having derived the acoustic energy from a single droplet, we can now use the result to predict the relation between the sound level in a rain shower and the rate of rainfall. To demonstrate this, we give a simple example where we assume that the shower contains acoustically energetic drops of identical size. Letting  $N$  denote the number of drops impacting on unit surface area within unit time, the rate of rainfall per unit time is then given by

$$R = \frac{4}{3}\pi a^3 N. \quad (4.7)$$

Since the acoustic energy radiated from a single droplet is given by (4.5), the energy from unit source area within unit time is simply  $E$  times  $N$ , provided that the drops are energetically decoupled from each other, which is very likely to be the case because drops in natural rains are sporadically and sparsely distributed. It can also be noted that, if the shower covers a large surface area, this amount of energy is actually the energy flux of sound in the far field, namely the sound intensity. Denoting it by  $I$ , we have from (4.6) that

$$I = \frac{1}{8}\rho_0 U^2 \pi a^3 M^3 N. \quad (4.8)$$

The combination of (4.7) and (4.8) then immediately yields the relation between the sound intensity  $I$  and the rainfall rate  $R$  as

$$I = \frac{3}{32}\rho_0 U^2 M^3 R, \quad (4.9)$$

which shows a linear dependence between the two, and is consistent with experimental observations (Scrimger *et al.* 1989). We have derived a similar result to (4.9) before from a general theory based on dimensional analysis (Guo 1986), where the theoretical predictions were compared with some available measurements (Nystuen 1986), which shows quite good consistency in both the functional dependence between the sound level and the rainfall rate and the absolute decibel levels. It should be pointed out that this simple example should be taken as no more than an illustration of how our theoretical development can be applied to predict rain noise; a more accurate prediction would require consideration of more factors that may well be important but are not taken into account here. These, among other things, include considering the drop size as a distribution instead of a single value, and the impact velocity as a function of the drop size. It should also be pointed out that the acoustic energy radiation predicted by the above theory is likely to be relevant to the high-frequency noise away from the spectral peak.

## 5. Conclusions

To see how sound is generated by the initial impact of a droplet falling onto an otherwise quiescent water surface, we have examined the flow and the radiated compressive waves due to the impact. It has been shown that the impact causes rapid momentum exchange between the falling fluid elements and those in the water body,

and that this exchange is accomplished by the radiation of compressive waves which escape to the far field as sound. The supersonically expanding contact circle between the drop surface and the water surface has been identified as the main source of compressive waves, because the momentum exchange is most rapid in the region close to the contact circle. When the expanding velocity of the contact circle becomes subsonic, some waves travel outwards horizontally to overtake the contact circle and energize the fluid elements ahead of the contact circle in both the droplet and the water body. This reduces the velocity difference between the two groups of fluid elements before the impact occurs, so that the momentum exchange after the impact is much more gradual and less significant acoustically.

The wave pattern produced by the initial impact has been derived analytically, and shows that the waves have amplitudes of the order  $\rho_0 Uc$ , in analogy with the phenomenon of the one-dimensional water hammer. In fact, we have shown that the impact is locally precisely a water hammer phenomenon; all of the waves are produced with amplitude exactly equal to  $\rho_0 Uc$ , but because the waves have to propagate away from their source in a three-dimensional space, and in doing so suffer from amplitude decrease due to spherical spreading, the observed impact pressure fluctuations are usually less than this value. It has been shown that the initial impact-generated waves form a wave packet with higher values close to its front edge. The far-field sound will then be heard as a noisy shock-like pulse of extremely short duration, followed by a tail of rapidly decreasing amplitude. The pressure-release boundary surfaces reflect some of the waves from the direct impact. These reflected waves have the opposite sign to the original waves so that the far-field sound pulse has a tail, probably decreasing to a negative value before its amplitude decays to zero, forming the complete cycle which has often been observed in both experiments and numerical simulations.

The pressure wave pattern has been given only for small time right after the impact. To examine the far-field radiation at large time, effects such as the reflection from the boundary surfaces would have to be taken into account, which appears to be a very difficult task. However, the acoustic energy that is expected to be radiated to the far field has been calculated analytically. This can be done because this amount of energy is actually equal to that carried by the waves at small time before they reach the far field, that is, before they undergo the reflection process. The reflection only changes the pressure wave form, but has no effect on the energy carried by the waves. We have shown that the acoustic energy from the impact of a single droplet is proportional to the kinetic energy carried by the drop and to the cube of the impact Mach number, a result which has also been obtained before from both experimental observations and theoretical studies. To demonstrate the possible application of our theoretical investigation to natural rain, we have given a simple example where the sound level from a rain shower is related to the rate of rainfall; this shows a linear dependence between the two. We have noted the consistency between the predicted results in this simple example and some available measurements in both functional dependence and actual decibel levels.

#### REFERENCES

- DOWLING, A. P. & FFWCS WILLIAMS, J. E. 1983 *Sound and Sources of Sound*. Ellis Horwood.  
 FRANZ, G. J. 1959 Splashes as sources of sound in liquids. *J. Acoust. Soc. Am.* **31**, 1080–1096.  
 GRADSHTEYN, I. S. & RYZHIK, I. M. 1980 *Tables of Integrals, Series, and Products*. Academic.  
 GUO, Y. P. 1986 Wave-induced sound in the ocean. Ph.D. thesis, University of Cambridge.

- JONES, D. S. 1982 *The Theory of Generalized Functions*. Cambridge University Press.
- LIGHTHILL, M. J. 1952 On sound generated aerodynamically: I. General theory. *Proc. R. Soc. Lond. A* **211**, 564–587.
- MINNAERT, M. 1933 On musical air-bubbles and the sounds of running water. *Phil. Mag.* **16**, 235–248.
- NYSTUEN, J. A. 1986 Rainfall measurements using underwater ambient noise. *J. Acoust. Soc. Am.* **79**, 972–982.
- OĞUZ, H. N. & PROSPERETTI, A. 1990 Bubble entrainment by the impact of drops on liquid surfaces. *J. Fluid Mech.* **219**, 143–179.
- PLESSET, M. S. & PROSPERETTI, A. 1977 Bubble dynamics and cavitation. *Ann. Rev. Fluid Mech.* **9**, 145–185.
- PROSPERETTI, A., CRUM, L. A. & PUMPHREY, H. C. 1989 The underwater noise of rain. *J. Geophys. Res.* **94**, 3255–3259.
- PUMPHREY, H. C., CRUM, L. A. & BJORNO, L. 1989 Underwater sound produced by individual drop impacts and rainfall. *J. Acoust. Soc. Am.* **85**, 1518–1526.
- SCRIMGER, J. A., EVANS, D. J., McBEAN, G. A., FARMER, D. M. & KERMAN, B. R. 1987 Underwater noise due to rain, hail, and snow. *J. Acoust. Soc. Am.* **81**, 79–86.
- STRASBERG, M. 1956 Gas bubbles as sources of sound in liquids. *J. Acoust. Soc. Am.* **28**, 20–26.
- WENZ, G. W. 1962 Acoustic ambient noise in the ocean: spectra and sources. *J. Acoust. Soc. Am.* **34**, 1936–1956.